Innovative Food Science and Emerging Technologies 86 (2023) 103362

Contents lists available at ScienceDirect

Innovative Food Science and Emerging Technologies

journal homepage: www.elsevier.com/locate/ifset

Temperature controlled cryoprinting of food for dysphagia patients

Leo Lou [a], Cristina Bilbao-Sainz [b,*], Delilah Wood [b], Boris Rubinsky [a,c]

[a] Department of Bioengineering, University of California Berkeley, Berkeley, CA 94720, USA
[b] U.S. Department of Agriculture, Western Regional Research Center, 800 Buchanan St., Albany, CA 94710, USA
[c] Department of Mechanical Engineering, University of California Berkeley, CA 94720, USA

ARTICLE INFO

Keywords:
3D cryoprinting
Temperature controlled cryoprinting
Dysphagia
Beef
Anisotropic texture
Microstructure

ABSTRACT

Temperature Controlled Cryoprinting (TCC), employs temperature-controlled freezing to generate a desired ice crystal microstructures in each printed voxel, to yield a 3D printed bioproduct with intended microstructure. We introduce the use of TCC, originally developed for tissue engineering, for food manufacturing. TCC was used to make a beef product with anisotropic texture, for people with dysphagia (food swallowing difficulties). The effects of printing, cross-linking order, and directional freezing rates on the microstructure, viscoelastic and textural properties of TCC beef, were examined. Scanning electron microscopy shows that when directional freezing occurred before cross-linking, the microstructure consists of anisotropic alternating ridges of beef material with elongated pores parallel to the freezing direction. Shear stress tests confirmed that the meat had solid-like behavior and textural anisotropy, a desirable property lacking in conventional isotropic dysphagia foods. International Dysphagia Diet Standardization Initiative tests categorize the TCC beef as level 6 (soft and bite-sized) food.

Industrial relevance: The TCC technology can be used to provide texture and anisotropic microstructure to a variety of isotropic food products, such as ground meat, alternative meat or synthetic meat. The TCC technology could be also used for one-step process that combines manufacturing and freezing of foods.

1. Introduction

1.1. Statistics of dysphagia patients

Food swallowing problems, a medical condition known as dysphagia, affects 1 of 6 adults in the United States (Barczi & Robbins, 2000). Dysphagia has been associated with increased mortality and morbidity as well as the deterioration in the quality of life (Sura, Madhavan, Carnaby, & Crary, 2012). It can lead to malnutrition, dehydration, weight loss, aspiration pneumonia, chocking and death (Mayo Clinic Sept 4, 2023). The incidents of dysphagia increase with age (Hollinghurst & Smithard, 2022), with an estimated 10% to 30% of those older than 65 years suffering from dysphagia (Barczi & Robbins, 2000). Also, studies show that up to 68% of elderly home residents, 30% of the elderly admitted to a hospital and between 13% and 38% of the elderly living alone suffer from dysphagia (Sura et al., 2012). Millions of people worldwide are affected by dysphagia, including the elderly and those suffering from stroke, neurological diseases and cancer, all of which also increase in prevalence with aging (Aslam & Vaezi, 2013). In addition, up to 64% of patients who had suffered a stroke experienced dysphagia (Sura et al., 2012).

1.2. Dysphagia diet

Feeding inappropriate foods to dysphagia patients can result in severe health complications and even death. To avoid these health complications, dysphagia patients are served foods with modified texture and consistency. Currently, the texture modified foods served to dysphagia patients include purees, minced or small bite-size forms or liquids. However, often, these foods are visually and textural unappetizing and nutritionally diluted (Germain, Dufresene, & Gray-Donald, 2006). Studies have shown that dysphagia patients placed on texture modification diets (puree) tend to have between 17%–37% lower energy intake than those on regular diets (Milles et al., 2019). These foods often lack carbohydrates and proteins (Milles et al., 2019), resulting in undernourished patients with a likely compromised immune system.

1.3. International dysphagia diet standardization initiative (IDDSI) test

It is recognized that texture is a key parameter for dysphagia foods

* Corresponding author.
E-mail address: cristina.bilbao@usda.gov (C. Bilbao-Sainz).

https://doi.org/10.1016/j.ifset.2023.103362
Received 5 January 2023; Received in revised form 7 April 2023; Accepted 8 April 2023
Available online 11 April 2023
1466-8564/Published by Elsevier Ltd.

(Raheem, Carrascosa, Ramos, Saraiva, & Raposo, 2021). A comprehensive review of the properties and technology of texture-modified foods for dysphagia patients is found in Raheem et al. (2021). The authors correctly state that "Today, the literature on the impacts of texture modified food, developed by food scientists, on food swallowing, remains scarce." In 2012, the International Dysphagia Diet Standardization Initiative (IDDSI) was founded to provide a globally standardized terminology and definitions for texture-modified food and liquids that are applicable to dysphagia individuals of all ages, in all care settings, and for all cultures (Cichero et al., 2017). IDDSI is currently the only texture-modified diet recognized by the Nutritional Care Manual®. The IDDSI defines eight different classes of foods for various levels of dysphagia in two categories, liquids from 0 to 4 and transitional foods from 5 to 7. Tests were recommended for each class of food. In this study, we will evaluate foods made with the technique of Temperature Controlled Cryoprinting (TCC) with IDDSI tests for food of categories 4 to 6. Since the IDDSI tests cannot capture the special properties of the foods made with the TCC technology, we add rheology tests and texture tests.

1.4. Novel foods for dysphagia

New manufacturing approaches are being developed to provide dysphagia patients with visually and texturally appealing nutritious foods. Food cast in a visually appealing mold had been shown to yield a substantial increase in food consumption over a food presented in conventional pureed form (Farrer, Olsen, Mousley, & Teo, 2016). There is increasing interest in using 3D printing in food manufacturing (D'Angelo, Hansen, & Hart, 2016; Liu, Zhang, Bhandari, & Wang, 2017; Mantihal, Kobun, & Lee, 2022; Sun, Peng, Yan, Fuh, & Hong, 2015; Yang, Zhang, & Bhandari, 2017). Recently, advances in 3D printing had led to their use in the production of dysphagia foods (Kouzani et al., 2017; Lorenz, Iskanfdar, Baeghbali, Ngadi, & Kubow, 2022). Currently, the main advantage of 3D printing of dysphagia food over casting is that it can take a more complex and visually appealing appearance. Unlike molding, it can also make foods with macroscale texture (Lipton, Cutler, Nigl, Cohen, & Lipson, 2015). However, current 3D printing of food in general and for dysphagia patients in particular cannot control the food texture at the microscale, an issue which the technology of this paper will address. For example, current 3D printing food technologies cannot make muscle-like foods with micro scale, muscle fiber-like anisotropic textures. A commonly used technique for 3D printing of foods for dysphagia patients employs inkjet printing technologies with inks made from a mixture of pureed foods, water, protein, starch, and other hydrocolloids. The hydrocolloids include those commonly used in the food industry for thickening purposes: cold swelling (xanthan gum and guar gum) and heat soluble (k-carrageenan and locust bean gum) (Dick, Bhandari, & Prakash, 2021. The technological issues with using these hydrocolloids in food manufacturing are similar to those encountered in 3D printing for tissue engineering applications. Mixing the printing ink with hydrocolloids increases the viscosity of the ink. Furthermore, adding cross-linkers can change the viscosity as a function of time. This leads to difficulties in controlling the viscosity of the printing ink when delivered from the printing nozzle orifice, as well as consistency in printing. Furthermore, the printed food products, with the exception of chocolate, is soft and without mechanical rigidity. This leads to difficulties in printing large and complex structures.

At the microscale foods can be isotropic or anisotropic. Isotropic foods, have uniform material properties in all directions. For example, gels or minced meat. Anisotropic foods have direction dependent material properties. Most tissues, especially meat have distinct anisotropic character (Oppen, Grossmann, & Weiss, 2022). The 3D food printing technologies reported in literature can make visually appealing products. However, at the microscale, the material properties and texture are isotropic. The 3D printing ink is made of mashed food and the printing process does not yield anisotropy at the microscale. This is one of the reasons the dysphagia patients report the food as boring. Conventional 3D printing cannot make products with anisotropic microscale structures in which the material properties and texture are direction dependent, such as the fibers along muscle tissue. Anisotropic microstructure is critical for producing a dysphagia food with texture. For example, a food that has a texture which resembles meat and muscle fibers. Conventional 3D printing is a slow process that can result in biological matter spoilage during printing (Lipton et al., 2015). The current 3D printing technology are not suitable for mass production, which is essential in the food industry. However, Temperature Controlled Cryoprinting (TCC), originally developed for tissue engineering, can overcome many of the drawbacks found in conventional 3D printing and should be particularly suitable for making foods with texture. A description of the TCC technology and the advantages over conventional 3D printing are discussed in Section 1.5.

1.5. Temperature controlled cryoprinting (TCC)

The TCC technology was originally developed for tissue engineering (Adamkiewicz & Rubinsky, 2015; Rubinsky, Adamkievicz, & Shaked, 2017; Ukpai et al., 2019; Ukpai & Rubinsky, 2020a, 2020b; Zawada, Ukpai, Powell-Palm, & Rubinsky, 2018). The key feature of TCC is temperature-controlled freezing of each 3D printed voxel, and immersion of the printed layer in a constant temperature fluid at subfreezing temperatures. In this way, the printed object is frozen as it is printed, with controlled cooling rates, and is maintained in a controlled frozen state until the object is completed. This has several advantages over conventional 3D printing. A) Freezing provides mechanical rigidity to the printed structure. This allows printing of highly complex structures, including cavities and overhangs made of soft food material (Zawada et al., 2018). B) Because the printed material is frozen, the product cannot deteriorate during the printing process. C) Because the temperature is precisely controlled during the freezing of each voxel, the ice crystal size throughout the entire food product is uniform and optimal for preservation (Warburton, Lou, & Rubinsky, 2022). D) Because the outcome of the TTC 3D cryoprinting is a frozen product, it is possible to make a frozen product for markets directly, instead of the conventional method of frozen foods manufacturing. Currently, in the food industry, frozen food is made by first making the food and then freezing it, usually with difficult to control cooling rates. E) Most relevant to the application in this paper is the fact that TTC can generate a controlled microstructure in each voxel of food, by controlling the freezing process. This is achieved by controlling the microscale structure of ice in voxel throughout the printed object. The concept draws from the crystallographic properties of ice. Ice has a tight crystallographic structure and cannot incorporate solutes. Therefore, during freezing of an aqueous solution, the solutes are rejected around the ice crystals, resulting in a microscale structure. This microstructure is retained after thawing (Preciado, Skandakumaran, Cohen, & Rubinsky, 2003). The size of the microstructure elements depends on the cooling rates and the direction of the temperature gradients during freezing (Rubinsky & Ikeda, 1985; Ukpai & Rubinsky, 2020a). One of the drawbacks of 3D printing is that it is designed for the manufacturing of one product on one device and is not suitable for mass manufacturing (Lipton et al., 2015). The TCC technology is amenable for mass manufacturing. The concept is described in Ukpai et al. (2019) and Zawada et al. (2018). The key aspect of the technology is that each 3D printed layer is frozen separately under temperature control. Therefore, the TCC technology consists of several independent steps, including printing a layer, freezing the layer, cross-linking the layer and assembling the layer into a 3D object. Because each step is independent of the others, it is possible to print multiple layers simultaneously and in parallel. A robotic arm can then be used to assemble each layer in the 3D structure. Freezing aids in the binding between the different layers. A detailed description of the robotic assembly process of TCC multilayers parallel printing is described in, Ukpai et al. (2019) and Zawada et al. (2018). Previous studies (Ukpai

et al., 2019; Ukpai & Rubinsky, 2020a; Zawada et al., 2018) showed that this technology can eliminate thousands of hours per m^3 of product manufacturing. To control the effect of various parameters in TCC and because the technology involves different devices that can operate in parallel, we have developed a system made of modular TCC elements. The modular elements are: a) 3D printing of a layer, b) controlled freezing of the layer, c) cross linking, and d) assembly. This design allows us to study separately the effect of every parameter in the TTC process (Warburton et al., 2022). In this study we use the modular TTC system (Warburton et al., 2022) in which each step of the TCC process is on a different device. The devices include a 2D printing unit, a cross-linking unit (Warburton & Rubinsky, 2022) and a directional solidification freezing unit (Warburton et al., 2022). We took advantage of the modular nature of the technology to study the effect of various parameters on the properties of the product, For a fundamental study on the effect of different parameters on the product it is possible to exchange the order of printing and cross-linking because the units are modular.

The goal of this study was to illustrate the potential use of the TCC technology in food manufacturing for patients with dysphagia. To this end, we created a 3D cryo-printed beef with anisotropic texture for patients suffering from dysphagia, as an alternative to conventional isotropic dysphagia food. We investigated the influence of cross-linking order (before or after directional freezing) and freezing rates (1 °C/s and 5 °C/min) on the microstructure, rheological and textural properties of the 3D cryo-printed meat, with emphasis on the suitability of the product for a dysphagia diet.

2. Materials and methods

2.1. Printing ink

Materials used for the dysphagia food ink are: sodium alginate (Sigma-Aldrich, Burlington, MA, USA), ground beef, 20% (*w*/w) fat (Schenk Packing Co Inc., Stanwood, WA, USA), calcium chloride (Fisher Scientific, Fairlawn, NJ, USA), deionized water (type II, Fisher Science, Hampton, NH, USA). The ground beef (300 g) was cooked in a microwave oven (Toshiba, Tokyo, Japan) using a 1100 W setting for 2 min. The ground beef was placed in a glass container and stirred every 30 s during the 2 min of microwave cooking. The cooked meat was mixed with 100 mL of a 5% w/w sodium alginate solution. Then, 50 mL of deionized (DI) water was added to the beef/sodium alginate mixture. After mixing, the ink was blended using a Ninja Professional Blender (Ninja, Needham, MA, USA) in the high-speed mode (19,000 rpm) for 3 min.

2.2. 3D temperature controlled cryoprinting (TCC) system

The TCC 3D printing system was a modified version of the modular 3D printing system described in Warburton et al. (2022). It consisted of three modular units: the printer, the cross-linking unit and the directional solidification unit. The printer generated the macroscopic features, the cross-linking unit was used to impart mechanical stability to the product and the directional freezing unit was used to generate the microstructure.

The 3D printing system was a modified Ender 3 3D Printer (Shenzhen Creality, Shenzhen, China) (Fig. 1A). An Arduino Mega 2560 Rev3 board (Arduino, Somerville, MA, US) replaced the original printer system. Marlin 2.0.9.3 was used as the firmware program (Scott, Roxanne, et al., 2022). The printing ink made from meat was viscous so the nozzle and extrusion system were redesigned for the meat printing application. The extrusion system is shown in Fig. 1B. Two NEMA 17 stepper motors (Iverntech, ShenZhen, China) were used to provide sufficient force for the extrusion process. The stepper motors were controlled by the TB 6600 stepper controller (Yisheng Technology, Hangzhou, China). The ink was housed in a 50 mL syringe (Fisher scientific, Hampton, NH, USA). The original nozzle was replaced with a specially designed 0.4 mm nozzle (Fig. 1C). The syringe was connected to the nozzle with a 1/2″ plastic tube (1/2" ID × 5/8"OD flexible plastic tubing).

A 2% crosslinking bath was prepared by dissolving 6 g $CaCl_2$ dehydrated powder in 300 mL of DI water using a stir bar. The cross-linking solution was transferred to a glass beaker, which served as the cross-linking bath unit. The cross-linking bath was kept at room temperature (23 °C) throughout the study. The samples were kept in the bath for 15 min at 23 °C. The samples were completely immersed in the $CaCl_2$ bath for 15 min at 23 °C, immediately after printing or immediately after being frozen.

The directional solidification system emulated the TCC system design in Warburton and Rubinsky (2022). The printed object was immersed in a bath filled with 45% ethylene glycol in water in such a way that there was a precisely controlled distance between the top surface of the fluid bath and each printed line. This facilitated temperature-controlled freezing of each voxel in each printed line

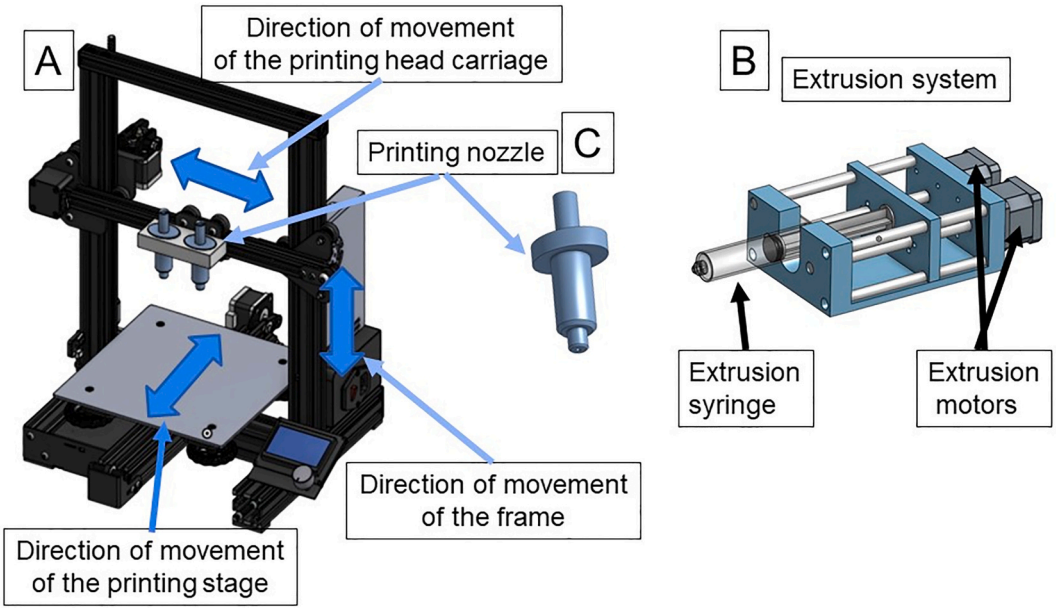

Fig. 1. Schematic representation of the 3D Printer (A), extrusion system (B) and printing nozzle (C).

(Ukpai et al., 2019; Ukpai & Rubinsky, 2020b). In this system, after a line was frozen, the sample was further immersed into the freezing fluid, as shown in Fig. 2A. In this design, every voxel in each printed line in the entire object was frozen with controlled freezing rates in a directional solidification process. Therefore, the voxels in the entire printed object experienced a uniform freezing rate and freezing direction, allowing control over the direction of ice crystal formation and the development of a microstructure. The constant freezing rate is calculated with the mathematical model described in (Ukpai et al., 2019; Ukpai & Rubinsky, 2020b) The entire printed sample went from room temperature (23 °C) to freezing bath temperature (−25 °C). The temperature was controlled using a refrigerated circulator (Nestlab RTE-140, Thermo Scientific, Waltham, MA).

To avoid contamination, the printed samples on the printing substrate were sealed in aluminum foil (Reynolds, Auckland, New Zealand) after carefully removing the air (Fig. 2B). The aluminum foil was connected to a syringe pump (Harvard Apparatus, Holington, MA) and immersed into the freezing fluid at a constant, controlled velocity. Two freezing rate settings were used in this study, slow freezing (5 °C/ min) indicated by the acronym SF and fast freezing (1 °C/s), indicated by the acronym FF.

The frozen samples were thawed in a cross-linking bath as described in Warburton and Rubinsky (2022). Briefly, the technology described in detail in that paper employs a technique in which a cross linker diffuses into the frozen material in tandem with the melting, so that the tissue structure is captured by the cross linking. After processing, the unfrozen TCC samples were sealed in zip-lock bags without air and kept in the refrigerator at 4 °C for further testing.

2.3. Scanning electron microscopy

Scanning electron microscopy (SEM) was performed using a Hitachi TM-4000 scanning electron microscope (Hitachi, Chiyoda City, Tokyo, Japan). The sample was first rapidly frozen by immersion in liquid nitrogen and then freeze-dried using a 4.5 L −50 °C freeze dryer (Labconco FreeZone, Kansas City, MO, USA) for 3 days.

2.4. Rheology

Rheological properties of the printing ink and the TCC printed products were determined using a DHR-3 rheometer (TA Instruments, New Castle, Delaware, USA) with a 20 mm steel plate (1 mm gap). The rheological properties of the printing ink could be used for the design of the printing head, whereas the rheological properties of the printed product was related to the chew/swallow characteristics of the food. The rheological properties were analyzed at 24 °C. The viscosity of the samples was measured as a function of shear rate from 0.11/s to 10 /s. Also, the storage modulus (G'), loss modulus(G") and damping factor ($\tan\delta$) of the samples were determined as a function of frequency from 0.1 to 100 rad/s at a constant strain of 0.2%. (Dick et al., 2021; Xing et al., 2022).

2.5. Texture properties

Texture properties of the printed samples were obtained using a TA. XT plus 100 texture analyzer (Stable Microsystems Ltd.,TA-XT2i,UK). Two different tests were performed: Texture Profile Analysis (TPA) and shear test. Both tests were conducted at room temperature (24 °C). TPA tests were used to mimic mastication behavior (Fig. 4A). TPA was obtained using a 7 mm cylinder probe. Samples were compressed 3 mm at 0.1 mm/s with a delay of 6 s between two compressions. The pre-test rate was 1.5 mm/s and the post-test rate was 10 mm/s. The tests were performed in triplicate (Dick et al., 2021; Xing et al., 2022). For the shear test, each sample was sheared to a depth of 3 mm at 0.1 mm/s using a TA-47 Lexan blade (Stable Microsystems Ltd., TA-XT2i, UK) (Fig. 4B). The peak force required to shear the sample was recorded during the last 1 mm during the shearing process. The samples were tested in two orthogonal directions relative to the blade. Five repeats were run for each sample.

2.6. International dysphagia diet standardization initiative (IDDSI) test

The IDDSI Test Methods were conducted on the 3D TCC samples cut into 2.5 cm × 2 cm × 0.5 cm pieces to categorize the texture-modified products based on the IDDSI Framework (International Dysphagia Diet Standardization Initiative, 2019). IDDSI is currently the only texture-modified diet recognized by the Nutritional Care Manual®. The IDDSI defined eight different classes of foods for various levels of dysphagia in two categories, liquids from 0 to 4 and transitional foods from 5 to 7. Tests were recommended for each class of food. Since the 3D TCC meat products were expected to be categorized in levels 4 to 7, the corresponding tests detailed in the IDDSI Framework were performed: fork pressure test, fork drip test and spoon tilt test. More specifically, for the fork pressure text, the sample was placed on a flat platform, pressure was then applied through the thumb of a house fork until the nails turned white and the denaturing properties of the samples were observed and recorded. For the fork drops test, the sample was placed on a fork and the flow behavior of the sample was observed and recorded. For the

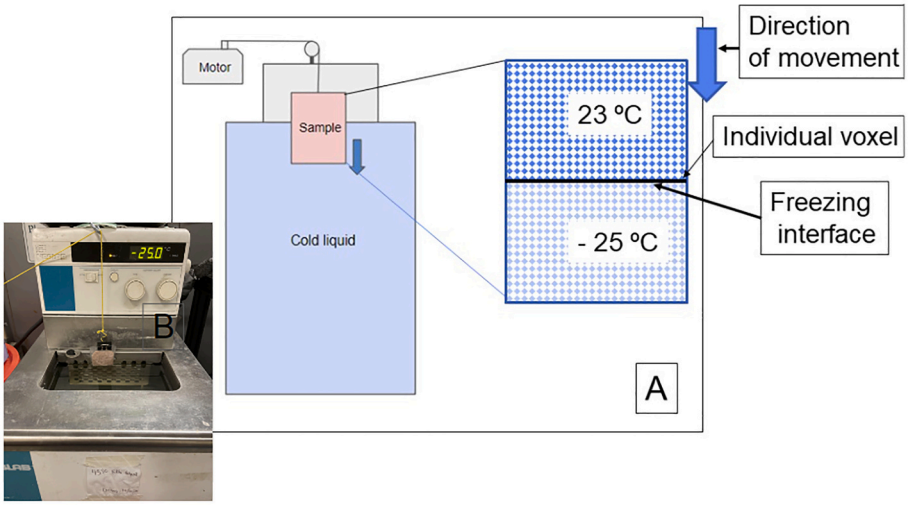

Fig. 2. A) Schematic representation of the directional freezing unit and B) sample preparation for directional freezing.

spoon tilt text, the sample was place on a spoon, the spoon was then slowly titled and the behavior of the sample during the process was observed and recorded.

2.7. Statistical analysis

One-way ANOVA and Duncan's multiple range test(DMRT) at 95% confidence level was used to compare different experimental groups in rheology, TPA and shear tests with SigmaPlot 14.0.

3. Results and discussion

3.1. Visual appearance

Fig. 3 illustrates the macroscopic appearance of the biological matter at two stages during the 3D TCC process. Panel 3A shows the appearance of the printing ink that was made from ground beef. This was the type of food puree often given to patients with dysphagia. Panel 3B shows the macroscopic appearance of a 3D printed beef slice using the printing ink shown in Panel 3A. This food product resembled a native beef slice.

3.2. Apparent viscosity of the printing ink

The printing ink had a high apparent viscosity (Fig. 4) compared with other 3D printing foods for a dysphagia diet (Dick et al., 2021; Xing et al., 2022) due to the use of a relatively high concentration of sodium alginate and low concentration of added water. High viscosity inks are a challenge for 3D printing since they clog the nozzle. However, the special design of the 3D printing extruder and nozzle (Fig. 1B and C) enabled printing of very viscous ink (up to ~10,000 Pa.s). The rheological properties of the 3D printing ink affected the ease of extrusion and the ability of the 3D printed sample to support itself before processing. In previous 3D printing studies, the cross-linker was added to the ink prior to printing, which could increase the viscosity of the ink and decreased the homogeneity of the printed product since cross-linking was continuously occurring during printing. For the 3D TCC technology, cross-linking occurred after printing, which allowed the use of a printing ink with high initial viscosity and the generation of a printed food product with homogeneous properties. The cross-linking after printing also provided the printed object with the consistency needed for the printed structure to remain intact. Therefore, the 3D TCC technology with the specially designed nozzle used in this study allowed the use of food inks with higher viscosities that would widen the variability of foods available for patients with dysphagia. From Fig. 4, the printing ink exhibited shear-thinning behavior, which was desirable for the 3D printing process. The viscosity at low shear rates was related to the material's property under low stress, such as phase separations and structure retention before and after extrusion. The viscosity at high shear rates corresponded to the flow-ability of the ink during extrusion since the material experienced high shear rates during extrusion through the nozzle (Liu et al., 2017). The shear thinning property was also

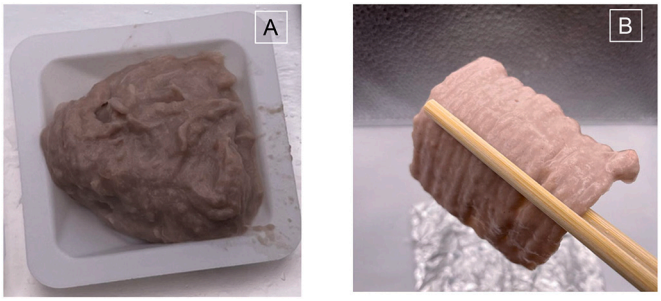

Fig. 3. A) Printing ink from cooked ground beef and sodium alginate and B) 3D TCC beef slice directionally frozen and cross-linked with $CaCl_2$.

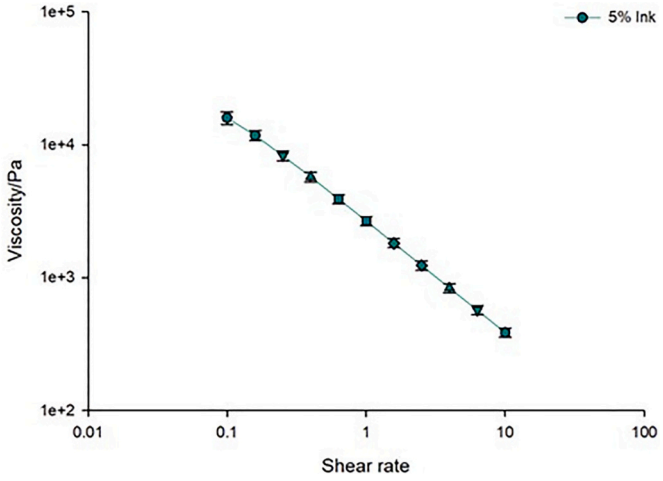

Fig. 4. Apparent viscosity as a function of shear rate of beef ink prepared with ground beef and 5% sodium alginate.

valuable for the dysphagia diet since the bolus could maintain its high viscosity at low shear and then easily flow and be swallowed after application of a high shear process such as chewing (Wei, Guo, Li, Ma, & Zhang, 2021).

3.3. Scanning electron microscopy (SEM)

Scanning electron microscopy was used to examine the microstructural variations that contributed to the textural and rheological properties of the printed samples. The network structure of the control sample appeared tight, indicating that the beef components might be interconnected with the calcium alginate to give a compacted appearance to the matrix (Fig. 5A-B). Also, the sample contained several holes that were attributed to occluded air bubbles in the beef matrix. Muscle myofibrils were not discernible since the main structures could have been destroyed during grinding through cutting and shearing (Berger, Witte, Terjung, Weiss, & Gibis, 2022). The microstructure changes in the CL-SF and CL-FF samples were mainly caused by the existence of ice crystals (Fig. 5C-F). Ice crystals randomly formed inside the tight cross-linked alginate-beef matrix and caused the meat grain matrix to appear broken. The microstructure became loose, rough and uneven with holes of different sizes. This effect was minimized when samples were frozen at a fast freezing rate (Fig. 5E-F) due to the formation of smaller and evenly distributed ice crystals (Mulot, Fatou-Toutie, Benkhelifa, Pathier, & Flick, 2019).

In comparison, the SF-CL and FF-CL samples had highly aligned directional microstructures parallel to the freezing direction, with regularly spaced ridges parallel to the ice growth direction alternating with elongated porous sections (Fig. 5G-J). Similar microstructures were previously reported during directional freezing of sodium alginate strands cross-linked with $CaCl_2$ (Warburton et al., 2022). In the absence of a cross-linking agent during directional freezing, ice crystals grew forward as a dendritic ice front, creating directional pores as the meat constituents were forced away. Upon thawing, the beef parts that were forced away from the ice front formed an extracellular matrix with a microstructure prescribed by the ice crystals that had formed during freezing. Previous authors had reported the effects of temperature control during freezing on the microstructure of ice (Rubinsky & Ikeda, 1985; Rubinsky, Lee, & Chaw, 1993;` Preciado et al., 2003; Ukpai & Rubinsky, 2020a; Zawada et al., 2018; Ukpai et al., 2019). An increase in the freezing rate from 5 °C/min to 1 °C/s resulted in a decrease in pore size from about 70 μm to about 10 μm, since higher freezing rates generated smaller ice crystals. It is important to note that the directional lines were uniform throughout the sample and occurred in the same direction. This was due to the use of 3D TCC, in which each voxel was

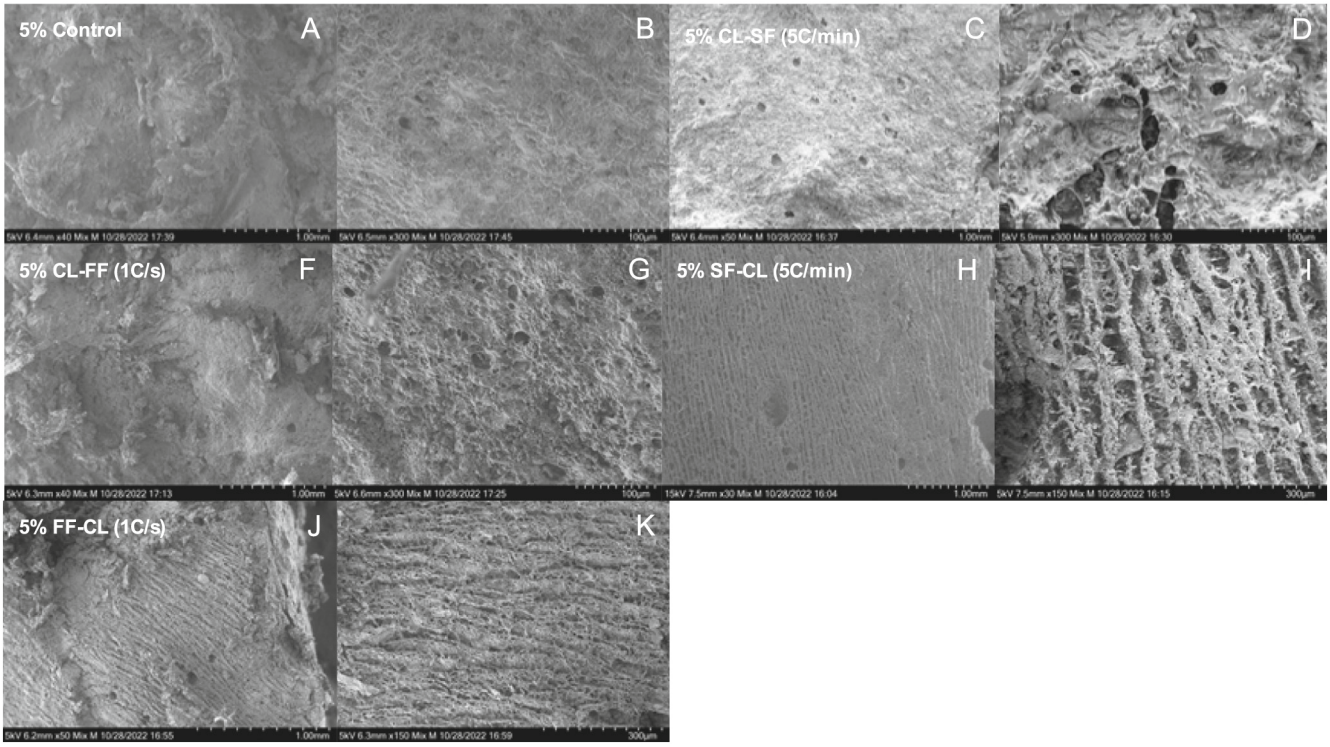

Fig. 5. Effects of cross-linking (CL) and freezing rate (slow freezing (SF) = 5 °C/min and fast freezing (FF) = 1 °C/s) on the microstructure of 3D temperature-controlled cryo-printed beef: Control (A and B), CL-SF (C and D), CL-FF (E and F), SF-CL (G and H) and FF-CL (I and J).

frozen with the same freezing rate and in the same direction, thereby generating a product with uniform properties. We have demonstrated that cryoprinting methods that controlled only the temperature of the printing base, or the temperature of the surrounding atmosphere could not generate a uniform and height-independent cryo-printed structure (Adamkiewicz & Rubinsky, 2015). These micrographs also showed that cross-linking after directional freezing could preserve the microstructures formed during freezing. This might be due to the cross linker diffusing into the frozen product in tandem with the melting process to fix the microstructure in place (Warburton & Rubinsky, 2022).

3.4. Dynamic viscoelastic properties

All printed samples had storage (G') and loss (G") moduli that increased in value with an increase in frequency (Fig. 6). In comparison, the ink had low moduli values that did not increase with frequency. For printed samples, the storage modulus was higher than the loss modulus throughout the frequency range, indicating that the materials had a more elastic rather than viscous behavior. This was due to the addition of sodium alginate cross-linked with $CaCl_2$ that resulted in the beef composite system becoming stiffer. Previous studies recommended that all gel foods designed for dysphagia patients should have comparable or higher G' values than G" values (Funami, 2011; Ishihara, Nakauma, Funami, Odake, & Nishinari, 2011). In this study, G' values of all printed samples ($\sim 10^5$ Pa) were one order of magnitude higher than the G" values ($\sim 10^4$ Pa). Fig. 6 also show that freezing increased the G' and G" values and increased the ability of the material to maintain its printed structure. (Liu et al., 2017; Zhao, Lin, & Zhou, 2017) also observed an increase in G' and G" values with freezing in alginate gels, which indicated that freezing and thawing promoted polymer associations that strengthened their structures. For samples that were first cross-linked and then frozen, slow freezing resulted in greater increases in G' and G" values compared with fast freezing. This could be related with fast freezing rates that minimized the disruption of the tissue in cross-linked samples (Fig. 5E-F). In comparison, samples that were first frozen and then cross-linked showed the opposite behavior. This can be related with a faster diffusion of the cross-linker during thawing when the air spaces are more homogenously distributed throughout the sample. Fig. 6 shows that all samples had tanδ values that ranged from 0.2 to 0.3. This indicated that the viscoelastic properties of the 3D TCC meat samples were within the safe range for dysphagia foods (Ishihara et al., 2011).

3.5. Shear stress test

The shear stress test was performed in two orthogonal directions, perpendicular and parallel to the freezing direction, to determine the degree of anisotropy in the printed samples. Fig. 7 shows that freezing significantly affected the shear force values in parallel (y) and perpendicular (x) to the freezing direction. The CL-SF sample had a slightly increased shear force value in the Y direction (7%) and in the X direction (9%) compared to the control sample. However, there were no significant differences between the parallel and perpendicular directions for Control, CL-SF and CL-FF, indicating isotropic behavior. This was consistent with the SEM images, which revealed no orientation in the freezing direction (Fig. 5C-D). The CL-FF sample had even larger increases in shear force values in the Y direction (21%) and in the X direction (29%). In comparison, the meat samples that were first frozen and then cross-linked showed the highest increases in shear force values. The SF-CL and FF-CL samples had increases in shear force values in the Y direction of 61% and 52%, respectively. These samples showed significantly greater increases in forces in the Y direction than in the X direction, which indicated the formation of anisotropic microstructures (Fig. 5G-J). These increases in shear force values could be due to the formation of dendritic elongated pores that provided faster diffusion for the cross-linker. Fig. 7 also shows that the cross-linker strengthened the material more in the direction parallel to the freezing direction than in the direction perpendicular to freezing direction. In addition, the SF-CL sample showed significantly higher shear force values than the FF-CL sample, which could be due to the formation of thicker ridges. The SF-CL and FF-CL samples had anisotropic structures that resembled the

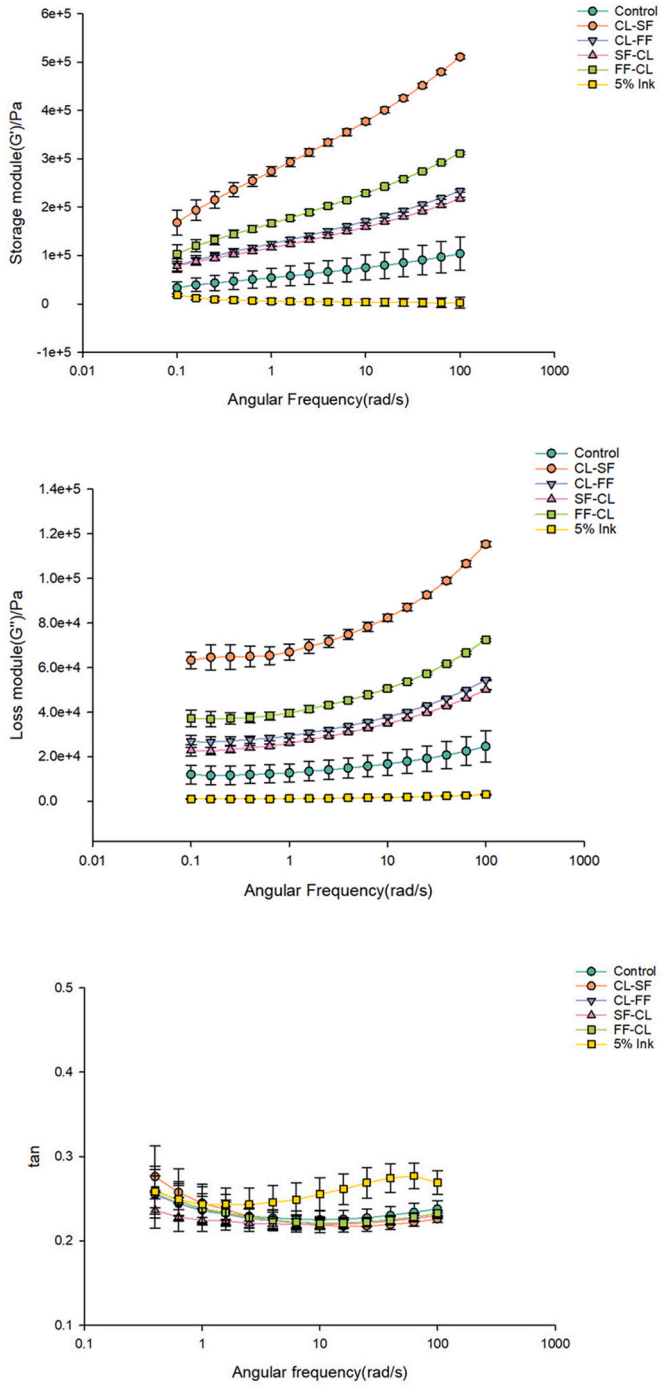

Fig. 6. Effects of the freezing rates (slow freezing = 5 °C/min and fast freezing = 1 °C/s) and the order of cross-linking (CL) and freezing on the dynamic viscoelastic properties of 3D TCC beef slices: Storage modulus (G'), Loss modulus (G") and Damping factor (tanδ).

anisotropic texture of real meat (Dekkers, Boom, & van der Goot, 2018), which was desirable in dysphagia foods (Tokifuji, Matsushima, Hachisuka, & Yoshioka, 2013). To summarize, TCC technology can print meat with specific anisotropic structures. This special function has not been shown by other 3D printing technologies for food applications.

3.6. Texture profile analysis (TPA)

One limitation in designing a proper texture-modified food for dysphagia patients is the lack of standards. (McCallum, 2003).The

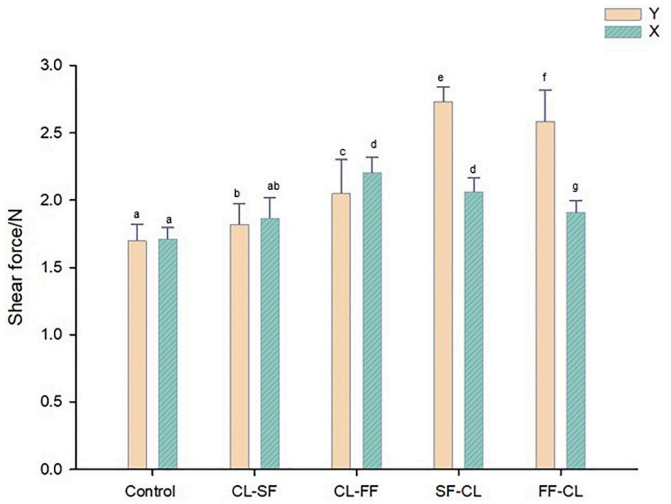

Fig. 7. A) Shear stress directions relative to freezing direction, and B) Effects of cross-linking (CL) and freezing rate (slow freezing (SF) = 5 °C/min and fast freezing (FF) = 1 °C/s) on shear force of 3D TCC beef slices.

National Dysphagia Diet had been proposed as an international dysphagia food classification, but did not include any texture parameters (McCallum, 2003).

Shear stress is a good measure of initial bite tenderness, but TPA provides more detailed information about the textural characteristics of foods (De Huidobro, Miguel, Blázquez, & Onega, 2005). The changes in adhesiveness, hardness, chewiness, gumminess, cohesiveness and springiness were used to evaluate texture characteristics of 3D TCC beef slices (Fig. 8). Adhesiveness, defined as the work needed to pull the testing probe away from the food sample during the first bite (Pons & Fiszman, 1996), may be the parameter of greatest importance when designing foods for dysphagia patients since adhesiveness is related to the feeling of swallowing difficulty. A higher adhesiveness would mean a longer time was needed for the food to leave the teeth and more difficulty in forming a bolus for swallowing (Park, Lee, Yoo, & Nam, 2020; Suebsaen, Suksatit, Kanha, & Laokuldilok, 2019).

Fig. 8A shows the adhesiveness of the different 3D TCC beef slices. Cross-linking of the meat samples led to an order of magnitude decrease in adhesiveness values relative to the ink sample from -100 g.*sec* to ~ −10 g.sec. It should be noted that the type of foods given to dysphagia patients often resembled the ink. Also, freezing led to a decrease in adhesiveness values. For example, the control sample had an adhesiveness value of −13.0 ± 4.5 g.sec. Whereas CL-SF, CL-FF, SF-CL and FF-CL had values of −9.2 ± 3.4 g.sec, −5.5 ± 1.3 g.sec, −10.8 ± 2.7 g.sec and − 9.7 ± 1.9 g.sec, respectively. Adhesiveness is a surface characteristic and depends on both adhesive and cohesive forces, viscosity and viscoelastic properties (Adhikari, Howes, Bhandari, & Truong, 2001). The decrease in adhesiveness due to freezing might be caused by enhanced cross-linking from directional freezing. Fig. 8A also shows that fast freezing resulted in lower adhesiveness values, which might be due to the formation of smaller pore sizes. Smaller pores that are created by the fast directional solidification may make the meat more porous, which decreases the surface contact area of the meat and leads to a smaller adhesiveness value (Yin et al., 2012). It should be noted that 3D TCC technology could generate uniform ice crystals throughout the entire structure. In contrast, freezing in conventional 3-D printing started from the exterior and proceeded inwards. In that case, the freezing rates decreased from the exterior to the interior and the adhesiveness in the external regions of the food should be lower than in the interior regions.

The hardness, defined as the maximum force required to compress the food in the first cycle (Pons & Fiszman, 1996; Rosenthal, 1999), significantly increased in value with freezing (Fig. 8B). This might be

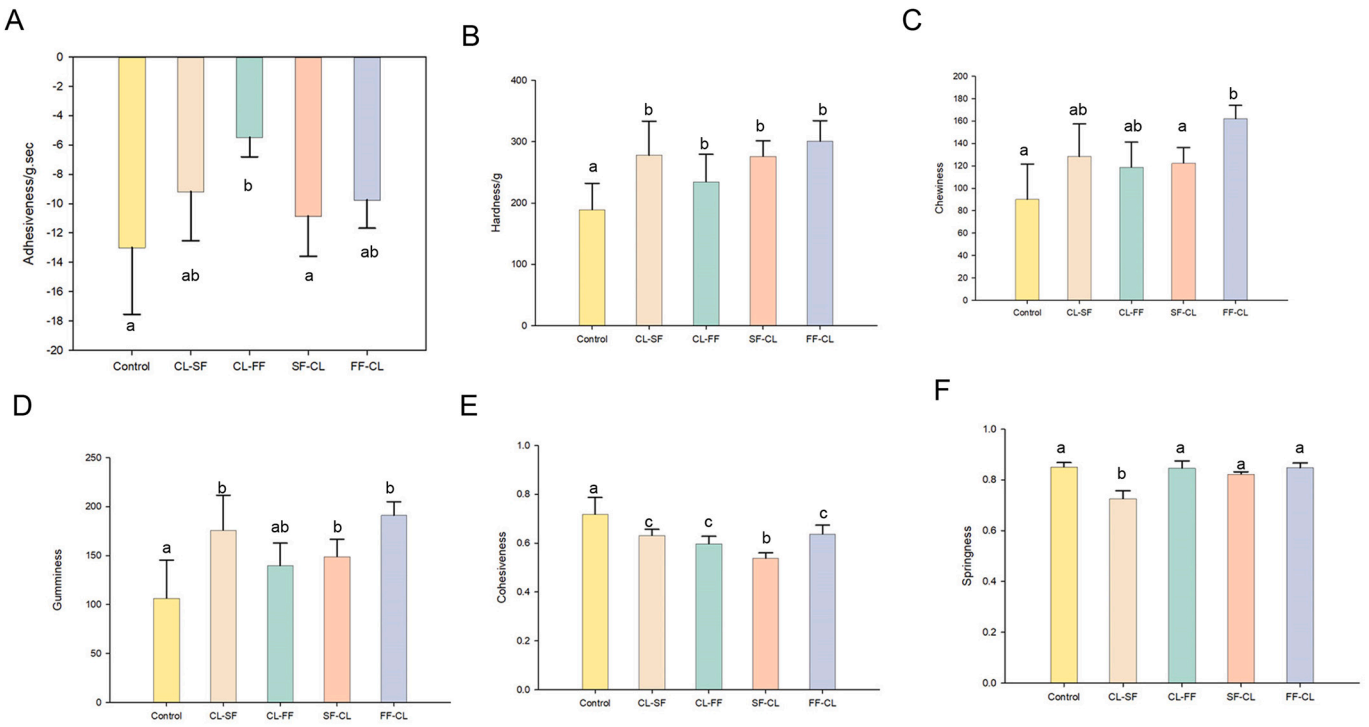

Fig. 8. Effects of cross-linking (CL) and freezing rates (slow freezing (SF) = 5 °C/min and fast freezing (FF) = 1 °C/s) on texture profile analysis (TPA) parameters of 3D TCC beef slices.

due to the highly porous microstructures generated during freezing that helped the migration of the cross-linking agent throughout the matrix and increased the samples' stiffness. Another possible explanation was the sublimation of ice crystals and dehydration of the samples. The chewiness and gumminess of the samples, which were related to hardness, also increased in value with freezing (Fig. 8C and Fig. 8D). Even with this increase, the 3D TCC beef slices had similar values to those found in previous studies on texture-modified food products for dysphagia patients (Dick et al., 2021; Xing et al., 2022). According to Spieker (2000), the dysphagia condition was related to the passage of the swallowed food through the throat or esophagus and not to chewing. Hardness was related to chewing dynamics and not directly related to swallowing dynamics (Momosaki, Abo, & Kobayashi, 2013). In any case, hardness was an important parameter related to the eating sensory feedback (Plesh, Bishop, & McCall, 1986), and was often neglected in the foods designed for the dysphagia diet. Similarly, chewiness and gumminess were related to the chewing process and played an important role in sensory perceptions, such as taste and mouthfeel. An increase in these parameters to some extent, while keeping them in the recommended ranges could provide foods with satisfactory textures (Mousavi, Heshmati, Daraei Garmakhany, Vahidinia, & Taheri, 2019).

The cohesiveness, defined as the internal bond that holds the food together (Rosenthal, 1999; Szczesniak, 1963), significantly decreased in value with freezing (Fig. 8E). This might be due to ice formation during freezing that weakened the beef and alginate network structure. A low cohesiveness value indicated the gels were more plastic than elastic, which was desirable for easy-to-chew foods (Zimoch-Korzycka et al., 2021). The cohesiveness values for the 3D TTC beef slices ranged from 0.5 to 0.6, which were within the range suggested by the Japanese Dysphagia Diet Criteria (*JDD2013*) defined by the Japanese Society of Dysphagia Rehabilitation (Matsuo & Fujishima, 2020). Also, all samples except CL-SF had comparable springiness values (Fig. 8F). The CL-SF sample had a significantly lower springiness value, indicating it had lower elasticity.

3.7. International dysphagia diet standardization initiative (IDDSI) test

The International Dysphagia Diet Standardization Initiative (IDDSI) (International Dysphagia Diet Standardization Initiative, 2019) was developed to facilitate readily accessible and internationally valid tests for dysphagia foods. It created "standardized terminology and definitions for texture-modified foods and thickened liquids to improve safety and care for more than 590 million people worldwide living with dysphagia" (Cichero et al., 2017).

This test was qualitative and recommended before the food was served to patients. The results of the fork pressure, fork drip and spoon tilt tests are summarized in Table 1.

For the fork pressure test, the ground beef sample became squashed, broke apart, changed shape and did not return to its original shape after removal of the fork. In comparison, some parts of the printing ink became tightly stuck to the fork. This suggested that the ink might be a potential choking hazard if it was served as food. Also, it was easy to push the fork through all the printed samples without thumb nail blanching, as prescribed by the IDDSI test. A clear pattern remained on these samples after removal of the fork and these samples did not adhere to the fork.

The results for the fork drip test showed that the printing ink gradually passed through the fork tines gap. In comparison, the printed samples remained on the fork and did not flow or drip through the fork tines.

The spoon tilt test is a practical way to evaluate the stickiness of the food. All samples except the printing ink dropped from the spoon when the spoon was tilted. The printing ink stuck to the spoon and gradually dropped off, which was consistent with the ink having a high adhesiveness value. A food that was too sticky could be a choking hazard since a greater lingual effect was required to move the food in and through the pharynx (Berzlanovich, Fazeny-Dörner, Waldhoer, Fasching, & Keil, 2005; Cichero et al., 2017). Thus, less sticky food was preferable for people with dysphagia. Cross-linking and directional freezing helped to hold the meat together and made it easier to slide off the spoon.

Overall, the ground beef could be classified as level 5 (minced and moist), the printing ink as level 4 (pureed) and the control, CL-SF, CL-FF, SF-CL and FF-CL samples as level 6 (soft and bite-sized) foods.

4. Conclusion

Modular 3D temperature-controlled cryo-printing (TCC) was used to manufacture 3D printed beef slices suitable for people with dysphagia. 3D TCC produced beef matrixes with viscoelastic solid behavior that conferred the desired consistency.

The order of manufacturing units significantly affected the properties of the printed beef. Microstructural analysis revealed that directional freezing before cross-linking resulted in ice crystals growing forward as a dendritic ice front and created directional pores intercalated with

Table 1
Results of the fork pressure test (A), fork drop test (B) and spoon tilt test (C) for ground beef, beef ink and 3D TCC beef slices. CL: Cross-Linking, SF: Slow Freezing (5 °C/min), FF: Fast Freezing (1 °C/s).

Sample	Fork pressure test	Fork drip test	Spoon tilt test	Comments
Control	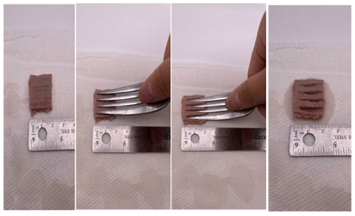 Description: It is easy to push with the fork. After pushing, parts of the sample were stuck to the fork. The imprint from the fork remained	 Description: No flow through the fork	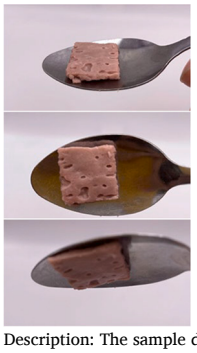 Description: The sample dropped as a whole when the spoon was flipped	Level 6 Soft and Bite-Sized
FF-CL	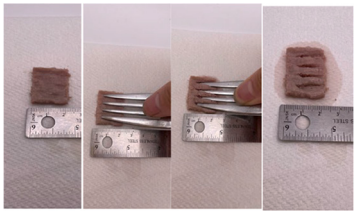 Description: It is easy to push with the fork. After pushing, the sample was a little bit stick to the fork. The imprint from the fork was clearly remained.	 Description: No flow through the fork	 Description: The sample dropped as a whole the spoon flipped	Level 6 Soft and Bite-Sized
CL-FF	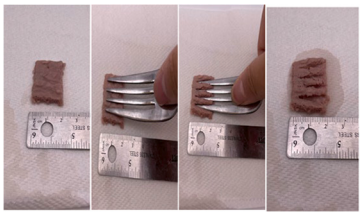 Description: It is easy to push with the fork. After pushing, the sample was a little bit stuck to the fork. The imprint from the fork was clearly remained	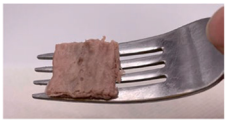 Description: No flow through the fork	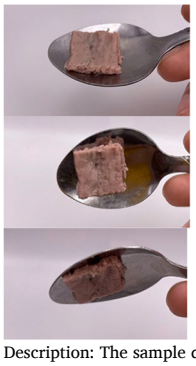 Description: The sample dropped as a whole the spoon flipped	Level 6 Soft and Bite-Sized
CL-SF	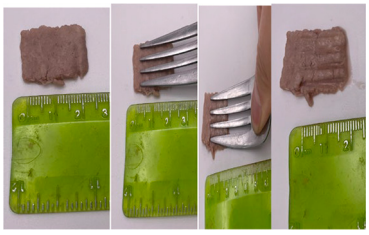 Description: It is easy to push with the fork. After pushing, the sample was a little bit stuck to the fork. The imprint from the fork was clearly remained	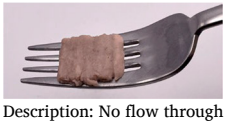 Description: No flow through the fork	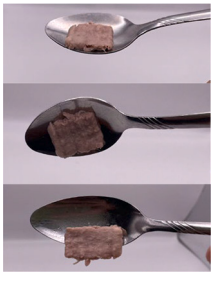	Level 6 Soft and Bite-Sized

(continued on next page)

Table 1 (*continued*)

Sample	Fork pressure test	Fork drip test	Spoon tilt test	Comments
SF-CL	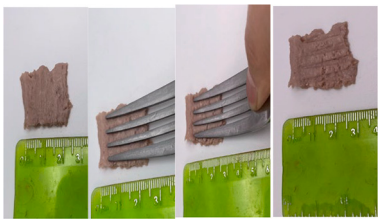 Description: It is easy to push with the fork. After pushing, the sample was a little bit stuck to the fork. The imprint from the fork was clearly remained	 Description: No flow through the fork	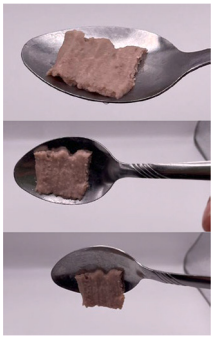	Level 6 Soft and Bite-Sized
Ink	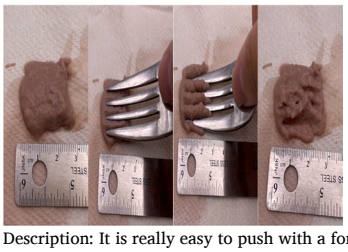 Description: It is really easy to push with a fork. The sample was very stuck to the fork and when the fork was removed, the imprint from the fork changed.	 Description: Ink could pile through the fork with a short tail below	 Description: The sample was quite sticky to slide off the spoon.	Level 4 Extremely thick
Ground Beef	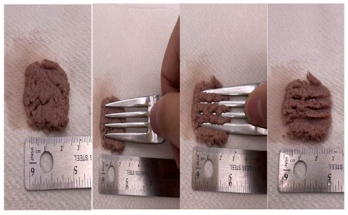 Description: It is easy to push with fork. The imprint from fork was remained after removing the fork	 Description: Sample can not pile through th fork	 Description: The sample was sticky but it can slide off the spoon	Level 5 Minced and Moist

homogenous ridges of beef material. This led to the generation of anisotropic structures that conferred texture to the 3D printed samples. The results of the stress forces measured parallel and perpendicular to the freezing direction confirmed the microscopic observations.

The microscopy, shear force and TPA results showed that freezing improved the desirable properties of beef slices for the dysphagia diet. Also, slow freezing before cross-linking was the most promising manufacturing process to create beef slices that especially appealed to consumers with dysphagia. These beef slices displayed the largest anisotropy ratio, reduced adhesiveness and cohesiveness and required less mastication effort (chewiness, gumminess) while keeping the initial bite tenderness (shear force) and hardness within the safe range for dysphagia foods. In addition, the 3D TCC beef slices satisfied the IDDSI requirements as level 6 foods for dysphagia patients.

CRediT authorship contribution statement

Leo Lou: Investigation, Methodology, Formal analysis, Data curation, Writing – original draft. **Cristina Bilbao-Sainz:** Methodology, Writing – review & editing, Supervision. **Delilah Wood:** Investigation. **Boris Rubinsky:** Conceptualization, Methodology, Writing – review & editing, Supervision, Project administration.

Declaration of Competing Interest

The authors declare that they have no known competing financial interests or personal relationships that could have appeared to influence the work reported in this paper.

Data availability

Data will be made available on request.

Acknowledgment

NSF Engineering Research Center for Advanced Technologies for Preservation of Biological Systems (ATP-Bio) NSF EEC#1941543.

References

Adamkiewicz, M., & Rubinsky, B. (2015). Cryogenic 3D printing for tissue engineering. *Cryobiology, 71*(3), 518–521. https://doi.org/10.1016/j.cryobiol.2015.10.152

Adhikari, B., Howes, T., Bhandari, B. R., & Truong, V. (2001). Stickiness in foods: A review of mechanisms and test methods. *International Journal of Food Properties, 4*(1), 1–33.

Aslam, M., & Vaezi, M. (2013). Dysphagia in elderly. *Gastroenterology & Hepatology, 9* (12), 784–795.
Barczi, S., & Robbins, J. (2000). How should dysphagia care of older adults differ? Establishing optimal practice patterns. *Seminars in Speech and Language, 21*(4), 347–361.
Berger, L. M., Witte, F., Terjung, N., Weiss, J., & Gibis, M. (2022). Influence of processing steps on structural, functional, and quality properties of beef hamburgers. *Applied Sciences, 12*(15), 7377. https://doi.org/10.3390/app12157377
Berzlanovich, A. M., Fazeny-Dörner, B., Waldhoer, T., Fasching, P., & Keil, W. (2005). Foreign body asphyxia: A preventable cause of death in the elderly. *American Journal of Preventive Medicine, 28*(1), 65–69.
Cichero, J., Lam, P., Steele, C. M., Hanson, B., Chen, J., Dantas, R. O., … Stanschus, S. (2017). Development of international terminology and definitions for texture-modified foods and thickened fluids used in dysphagia management: The IDDSI Framewprk. *Dysphagia, 32*, 293–314.
D'Angelo, G., Hansen, H. N., & Hart, A. J. (2016). Molecular gastronomy meets 3D printing: Layered construction via reverse Spherification. *3d Printing and Additive Manufacturing, 3*(3), 152–159. https://doi.org/10.1089/3dp.2016.0024
De Huidobro, F. R., Miguel, E., Blázquez, B., & Onega, E. (2005). A comparison between two methods (Warner–Bratzler and texture profile analysis) for testing either raw meat or cooked meat. *Meat Science, 69*(3), 527–536.
Dekkers, B. L., Boom, R. M., & van der Goot, A. J. (2018). Structuring processes for meat analogues. *Trends in Food Science & Technology, 81*, 25–36.
Dick, A., Bhandari, B., & Prakash, S. (2021). Printability and textural assesment of modified texture cooked beef pastes for dysphagia patients. *Future Foods, 3*, Article 100006.
Farrer, O., Olsen, C., Mousley, K., & Teo, E. (2016). Does presentation of smooth pureed meals improve patients consumption in an acute care setting: A pilot study. *Nutrition and Dietetics, 73*, 405–409.
Funami, T. (2011). Next target for food hydrocolloid studies: Texture design of foods using hydrocolloid technology. *Food Hydrocolloids, 25*(8), 1904–1914.
Germain, I., Dufresene, T., & Gray-Donald, K. (2006). A novel dysphagia diet improves the nutrient intake of institutionalized elders. *Journal of Americam Dietetic Association, 106*(10), 1614–1623.
Hollinghurst, J., & Smithard, D. G. (2022). Identifying dysphagia and demographic associations in older adults using electronic health records: A National Longitudinal Observational Study in Wales (United Kingdom) 2008–2018. *Dysphagia*. https://doi.org/10.1007/s00455-022-10425-5
International Dysphagia Diet Standardization Initiative. (2019). https://iddsi.org/framework/.
Ishihara, S., Nakauma, M., Funami, T., Odake, S., & Nishinari, K. (2011). Viscoelastic and fragmentation characters of model bolus from polysaccharide gels after instrumental mastication. *Food Hydrocolloids, 25*(5), 1210–1218.
Kouzani, A. Z., Adams, S., Whyte, D. J., Oliver, R., Hemsley, B., Palmer, S., & Balandin, S. (2017). 3D printing of food for people with swallowing difficulties. In *DesTech Conference Proceeding*. https://doi.org/10.18502/keg.v2i2.591
Lipton, J., Cutler, M., Nigl, F., Cohen, D., & Lipson, H. (2015). Additive manufacturing for the food industry. *Trends in Food Science &Technology, 43*(1), 114–123. https://doi.org/10.1016/j.tifs.2015.02.004
Liu, Z., Zhang, M., Bhandari, B., & Wang, Y. (2017). 3D printing: Printing precision and application in food sector. *Trends in Food Science and Technology, 69*, 83–94. https://doi.org/10.1016/j.tifs.2017.08.018
Lorenz, T., Iskanfdar, M. M., Baeghbali, V., Ngadi, M. O., & Kubow, S. (2022). 3D food printing applications related to dysphagia: A narrative review. *Foods, 11*, 1789, foods 11121789.
Mantihal, S., Kobun, R., & Lee, B.-B. (2022). 3D food printing of as the new way of preparing food: A review. *International Journal of Gastronomy and Food Science, 22*, Article 100260. https://doi.org/10.1016/j.ijgfs.2020.100260
Matsuo, K., & Fujishima, I. (2020). Textural changes by mastication and proper food texture for patients with oropharyngeal dysphagia. *Nutrients, 12*(6), 1613. https://doi.org/10.3390/nu12061613, 30.
Mayo Clinic Sept 4. (2023). https://www.mayoclinic.org/diseases-conditions/dysphagia/symptoms-causes/syc-20372028.
McCallum, S. L. (2003). The national dysphagia diet: Implementation at a regional rehabilitation center and hospital system.(solution center). *Journal of the American Dietetic Association, 103*(3), 381–385.
Milles, A., Liang, V., Sekula, J., Broadmore, S., Owen, P., & Braakhuis, A. J. (2019). Texture-modified diets in aged care facilities: Nutrition, swallow safety and mealtime experience. *Australasioan Journal of Ageing, 39*(1), 31–39.
Momosaki, R., Abo, M., & Kobayashi, K. (2013). Swallowing analysis for semisolid food texture in poststroke dysphagic patients. *Journal of Stroke and Cerebrovascular Diseases, 22*(3), 267–270.
Mousavi, M., Heshmati, A., Daraei Garmakhany, A., Vahidinia, A., & Taheri, M. (2019). Texture and sensory characterization of functional yogurt supplemented with flaxseed during cold storage. *Food Science & Nutrition, 7*(3), 907–917.
Mulot, V., Fatou-Toutie, N., Benkhelifa, H., Pathier, D., & Flick, D. (2019). Investigating the effect of freezing operating conditions on microstructure of frozen minced beef using an innovative X-ray micro-computed tomography method. *Journal of Food Engineering, 262*, 13–21. https://doi.org/10.1016/j.jfoodeng.2019.05.014
Oppen, D., Grossmann, L., & Weiss, J. (2022). Insights into characterizing and producing anisotropic food structures. *Critical Reviews in Food Science and Nutrition*, 1–19.
Park, J. W., Lee, S., Yoo, B., & Nam, K. (2020). Effects of texture properties of semi-solid food on the sensory test for pharyngeal swallowing effort in the older adults. *BMC Geriatrics, 20*, 1–5.
Plesh, O., Bishop, B., & McCall, W. (1986). Effect of gum hardness on chewing pattern. *Experimental Neurology, 92*(3), 502–512.
Pons, M., & Fiszman, S. M. (1996). Instrumental texture profile analysis with particular reference to gelled systems. *Journal of Texture Studies, 27*(6), 597–624.
Preciado, J. A., Skandakumaran, P., Cohen, S., & Rubinsky, B. (2003). Utilization of directional freezing for the construction of tissue engineering scaffolds. *Heat Transfer, 4*(4), 439–442. https://doi.org/10.1115/IMECE2003-42067
Raheem, D., Carrascosa, C., Ramos, F., Saraiva, A., & Raposo, A. (2021). Texture-modified food for dysphagia patients: A comprehensive review. *International Journal of Environmental Research and Public Health, 18*, 5125. https://doi.org/10.3390/ijerph18105125
Rosenthal, A. J. (1999). Relation between instrumental and sensory measures of food texture. *Food Texture: Measurement and Perception*, 1–17.
Rubinsky, B., Adamkievicz, M., & Shaked, Z. (2017). *System aparatus and methods for cryogenic 3D printing*.
Rubinsky, B., & Ikeda, M. (1985). A cryomicroscope using directional solidification for the controlled freezing of biological material. *Cryobiology, 22*(1), 55–68. https://doi.org/10.1016/0011-2240(85)90008-2
Rubinsky, B., Lee, C., & Chaw, M. (1993). Experimental observations and theoretical studies on solidification processes in saline solutions. *Experimental Thermal and Fluid Science, 6*(2), 157–167. https://doi.org/10.1016/0894-1777(93)90025-E
Scott, L., Roxanne, N., et al. (2022). *No Title. MarlinFirmware 2.0.9.3 Sourcecode*.
Spieker, M. R. (2000). Evaluating dysphagia. *American Family Physician, 61*(12), 3639–3648.
Suebsaen, K., Suksatit, B., Kanha, N., & Laokuldilok, T. (2019). Instrumental characterization of banana dessert gels for the elderly with dysphagia. *Food Bioscience, 32*, Article 100477.
Sun, J., Peng, Z., Yan, L., Fuh, J., & Hong, G. S. (2015). 3D food printing—An innovative way of mass customization in food fabrication. *International Journal of Bioprinting, 1* (1), 27–38. https://doi.org/10.18063/IJB.2015.01.006
Sura, L., Madhavan, A., Carnaby, G., & Crary, M. A. (2012). Dysphagia in the elderly: Management and nutritional considerations. *Clinical Intervertion in Aging, 7*, 287–298.
Szczesniak, A. S. (1963). Classification of textural characteristics a. *Journal of Food Science, 28*(4), 385–389.
Tokifuji, A., Matsushima, Y., Hachisuka, K., & Yoshioka, K. (2013). Texture, sensory and swallowing characteristics of high-pressure-heat-treated pork meat gel as a dysphagia diet. *Meat Science, 93*(4), 843–848.
Ukpai, G., & Rubinsky, B. (2020a). A mathematical analysis of directional solidification of aqueous solutions. *Journal of Heat Transfer, 142*(2). https://doi.org/10.1115/1.4045312, 022401–1.
Ukpai, G., & Rubinsky, B. (2020b). A three-dimensional model for analysis and control of phase change phenomena during 3D printing of biological tissue. *Bioprinting, 18*, Article e00077. https://doi.org/10.1016/j.bprint.2020.e00077
Ukpai, G., Sahyoun, J., Stuart, R., Wang, S., Xiao, Z., & Rubinsky, B. (2019). A parallel multiple layer cryolithography device for the manufacture of biological material for tissue engineering. *Journal of Medical Devices, Transactions of the ASME, 13*(3). https://doi.org/10.1115/1.4043080, 035001–1.
Warburton, L., Lou, L., & Rubinsky, B. (2022). A modular three dimensional bioprinter for printing porous scaffolds for tissue engineering. *Journal of Heat Transfer; ASME Transactions, 144*, 031205–1.
Warburton, L., & Rubinsky, B. (2022). Freezing modulated crosslinking: A crosslinking approach for 3D cryoprinting. *Bioprinting, 27*, Article e00225.
Wei, Y., Guo, Y., Li, R., Ma, A., & Zhang, H. (2021). Rheological characterization of polysaccharide thickeners oriented for dysphagia management: Carboxymethylated curdlan, konjac glucomannan and their mixtures compared to xanthan gum. *Food Hydrocolloids, 110*, Article 106198. https://doi.org/10.1016/j.foodhyd.2020.106198
Xing, X., Chitrakar, B., Hati, S., Xie, S., Li, H., Li, C., & Mo, H. (2022). Development of black fungus-based 3D printed foods as dysphagia diet: Effect of gums incorporation. *Food Hydrocolloids, 123*, Article 107173.
Yang, F., Zhang, M., & Bhandari, B. (2017). Recent development in 3D food printing. *Critical Reviews in Food Science and Nutrition, 3145–3153*. https://doi.org/10.1080/10408398.2015.1094732
Yin, M., Liu, M., Cao, Q., Wu, J., Tao, L., & Liu, J. (2012). Effect of pre-freezing rate on porosity ratio and mechanical property of pig aorta. *Frontiers in Bioscience-Landmark, 17*(2), 575–582.
Zawada, B., Ukpai, G., Powell-Palm, M. J., & Rubinsky, B. (2018). Multi-layer cryolithography for additive manufacturing. *Progress in Additive Manufacturing, 3*(4), 245–255.
Zhao, G., Lin, D., & Zhou, C. (2017). Thermal Analysis of Directional Freezing Based Graphene Aerogel Three-Dimensional Printing Process. *ASME Journal of Micro and Nano-Manufacturing, 6*(1), Article 011006. https://doi.org/10.1115/1.4038452
Zimoch-Korzycka, A., Kulig, D., Król-Kilińska, Ż., Żarowska, B., Bobak, Ł., & Jarmoluk, A. (2021). Biophysico-chemical properties of alginate oligomers obtained by acid and oxidation Depolymerization. *Polymers, 13*(14), 2258. https://doi.org/10.3390/polym13142258